National University of Singapore

Department of Chemical & Biomolecular Engineering

CN4123 DESIGN PROJECT

Individual Section Report

AY 2016/2017 Semester 2

Methanol-to-Olefins Plant

MTO Reactor Section

Student:	Timothy Ng Tik Ti
Matriculation Number:	A0110716U
Team:	10
Supervisor:	Professor Kawi
Date:	23rd March 2017

Executive Summary

The design of a Methanol to Olefins (MTO) reactor section to produce light olefins as part of a MTO plant was proposed. The MTO reactor section has a yearly production capacity of 882.6 kiloton/annum of light olefins from a feed (99.6wt% methanol, 0.4wt% water) of 3161 kiloton/annum.

A bubbling fluidized bed model was undertaken and the kinetics of the reactions was obtained from literature to simulate the reaction process. The catalyst used for the MTO reactions is chosen to be ZSM-5 zeolite, with its parameters taken as according to the literature with some modification to the particle diameter. A recycle stream containing methanol and dimethyl ether was found to have increased the methanol conversion from 85.2% to 98.2% using the optimized parameters of temperature, pressure and weighted hourly space velocity (WHSV).

Using the optimized parameters, the process variables of the reactor that could meet the specification of plant capacity and increased profitability were determined:

Table 1: Optimized Process Variables

Process Variables	
Reactor Volume	451.7m^3
Reactor Diameter	9.915m
Operating Temperature	550^oC
Operating Pressure	30atm
WHSV	134h^{-1}
Feed Rate	3161kt/a
Plant Capacity	882.6kt/a
Methanol Conversion	98.2%

The reactor and the equipment within the section were sized and estimated for their cost. The operating expenditure (OPEX) of the reactor section was found to be **$1.238E+09**, and the capital expenditure (CAPEX) was found to be **$8.470E+07**.

Contents

1. Introduction

The Methanol to Olefins (MTO) process was first discovered at Mobil Oil in 1977, which was found to be able to convert methanol to products such as olefins and gasoline. The MTO process converts methanol to light olefins such as ethylene and propylene, which have applications such as plastic manufacturing (Wang et al., 2006).

MTO process typically utilizes acidic zeolite catalysts such as SAPO-34 and ZSM-5, which have regular pore structure and size, and selectively allow certain chemicals in or out of the pores, providing selectivity to the olefin products. These catalysts speed up the MTO process and without them, the process would be too slow to be economically viable (Wang et al., 2006).

In this section report, the design of a reactor for the MTO reaction to produce olefins would be discussed in greater detail. A bubbling fluidized bed reactor was chosen to be our reactor of choice and was designed to hit the target specification of 800 kilotons of light olefin plant capacity per year. In addition, the equipment and the cost required to operate the reactor section would be examined as well.

2. Process Objective

In our process plant design, it is our objective to design a MTO plant to produce olefins, in particular ethylene and propylene, from methanol by using a solid catalyst. The plant would be situated in Singapore, and has an operation time of 8000 hours per annum. It is a requirement to produce 800 kiloton/annum of light olefins (ethylene and propylene) using a methanol feed of 99.6wt% purity, with water as an impurity. The plant would be designed in 7 different sections namely: 1) MTO reactor, 2) Water Removal, 3) De-C1, 4) De-C2, 5) De-C3, 6) De-C4, 7) Heat Integration

The MTO reactor would be the focus of this section report. As such, the objective of this report is to design a methanol-to-olefins (MTO) reactor section as part of the chemical plant that is capable of producing light olefins from methanol. The MTO reactor is the first unit of the chemical plant production process, with feed streams of fresh methanol. The amount of methanol feed would be ensured to achieve the required production capacity of light olefins, and the capacity of light olefins produced from the reactor should be higher than the requirement of 800 kt/a in order to account for the amounts lost during purification and separation steps in subsequent plant process. In order to maximize the conversion of methanol, excess methanol would be recovered and recycled. The design process would involve

modelling the MTO reactions and selecting optimal reaction parameters as well as design based on cost and production capacity.

3. Process Modelling

For the process modelling of our MTO reactor, we have decided to use a bubbling fluidized bed design. The bubbling fluidized bed was simulated with MATLAB R2016a, by utilizing reaction kinetics from Kaarsholm et al., (2010) and hydrodynamic correlations for a bubbling fluidized bed in order to obtain flow rates and composition of our product stream. Energy requirements of our reactor, streams, as well as auxiliary equipment were obtained from Aspen HYSYS v9.

3.1 Reaction Kinetics

Kaarsholm et al., (2010) in a study to model a set of kinetics for methanol to olefin reactions using ZSM-5 catalyst, ran multiple experiments considering different temperature, feed composition, catalyst mass to obtain experimental data on the composition and distribution of carbon species generated from the MTO reaction. From the data, a set of reaction kinetics was modelled and proposed by them. The kinetics obtained from the study was utilized in our own simulation with some modifications.

One modification made was an additional equation to describe the equilibrium between methanol and dimethyl ether. To do so, an additional kinetic equation was obtained from another study by Kaarsholm et al., (2011) to describe the rate of equilibrium reaction.

$$-r_{\mathrm{MeOH}} = \frac{kC_{\mathrm{M}}^2\left(1 - \frac{C_{\mathrm{D}}C_{\mathrm{W}}}{C_{\mathrm{M}}^2 K_{\mathrm{eq}}}\right)}{(1 + K_{\mathrm{M}}C_{\mathrm{M}} + K_{\mathrm{W}}C_{\mathrm{W}})^2}$$

where k is the forward rate constant, E_a is the activation energy for the forward reaction, K_m is the methanol constant and K_w is the water constant. C refer to component molar concentration.

As instructed during our design brief, another modification was made for the rate constant k_0 of equation 15 of the kinetics in Table A, which was changed from 3.46 to 0.5. In addition, equation 14 was removed entirely as well. The hydrocarbon intermediate, C_x, mentioned in the literature was taken and assumed to be $C_{10}H_{20}$ in our simulations.

As acknowledged by Kaarsholm et al., this kinetics model is able to simulate the overall trends of light olefins well. However, it is poor in simulating trends for paraffins and heavier olefins

fractions, especially hexene, and requires improvement in representing species concentration. It is also poor in simulating oxygenate conversion due to the lack of aromatics present in the kinetics, leading to a huge quantity of water being generated. In addition, this model was found to be accurate from a temperature range of 450 ^{o}C to 550 ^{o}C, and this meant that investigations outside this range could not be performed without sacrificing much accuracy. As such, these limitations would have to be acknowledged during our discussions on parameter design.

Due to the fact that ethane and propane are not included within the kinetics used, to improve our overall plant simulation, ethane and propane were introduced manually in Aspen HYSYS v9 to the outlet of the fluidized bed reactor.

3.2 Bubbling fluidized bed model

In order to simulate a bubbling fluidized bed, the two-phase model documented by Kunii and Levenspiel (1997) was used. This model assumes reaction takes place in the emulsion phase, and gas rises predominantly in the bubble phase and that interphase mass transfer occurs between the two. The fluidized bed of this model can be described using mass balance design equations around bubble and emulsion phases using a block element approach, utilizing the number of blocks as a parameter. Figure 1 below shows an illustration of the block element approach by Kaarsholm et al.

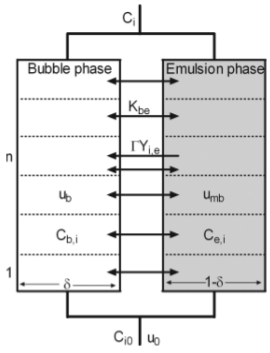

Figure 1: Block element approach by Kaarsholm et al

The design equations were given by Kaarsholm et al, to be:

$$0 = -F_{b,n}y_{b,i,n} + F_{b,n-1}y_{b,i,n-1} - \frac{\delta}{1-\delta}V_e K_{be}(C_{b,i,n} - C_{e,i,n}) + \sum_i^N (W_n(-r_i)) \cdot \frac{y_{e,i,n}}{1 - y_{e,C_x^1,n}}$$

$$0 = -F_{e,n}y_{e,i,n} + F_{e,n-1}y_{b,i,n-1} + \frac{\delta}{1-\delta}V_e K_{be}(C_{b,i,n} - C_{e,i,n}) - \sum_i^N (W_n(-r_i)) \cdot \frac{y_{e,i,n}}{1 - y_{e,C_x^1,n}} + W_n(-r_i)$$

where F_e and F_b are molar flow in emulsion phase and bubble phase respectively, y_e and y_b are molar fraction in emulsion and bubble phase respectively, δ is the bubble fraction, V_e is the volume of emulsion phase per stage, W_n is the weight of catalyst per stage, C_e and C_b are concentration of species in emulsion bubble phase respectively, and r_i is the rate equation with respect to the species. The assumptions of the design equations were as such:

1. Gas flows only in the axial direction, and dispersion in the radial direction is not considered
2. No catalyst present in the bubble phase
3. Activity of the catalyst is considered constant

In order to calculate the bubble fraction and bubble to emulsion mass transfer coefficient, hydrodynamic correlations for Geldart A powder classification were obtained from the same study and utilized.

By solving the design equations, it would be possible to obtain the flow rate of each component product, and as a result, key process specifications such as the plant capacity. Figure 2 below shows a flowchart to the methodology utilized by our MATLAB code in solving the design equations, and subsequently simulation in Aspen HYSYS.

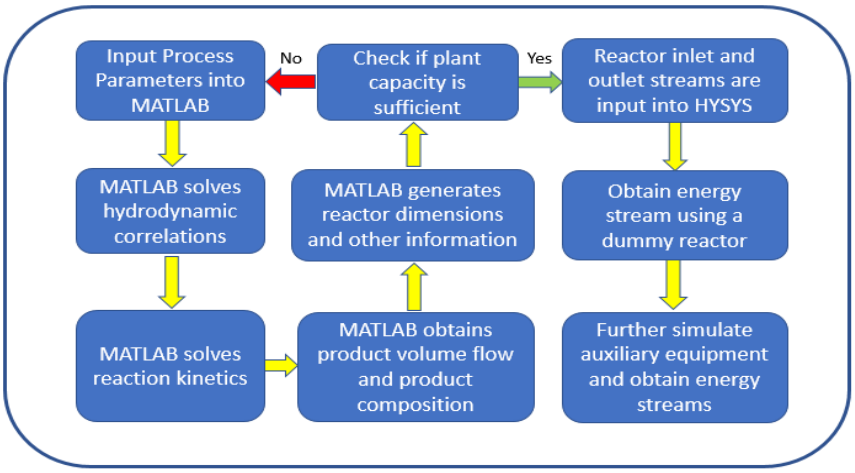

Figure 2: Flowchart of methodology of fluidized bed simulation

3.2.1 Additional assumptions of the model

In addition to the aforementioned assumptions, additional assumptions have been utilized in our model simulation. The additional assumptions are as follow:

1. Reactor is isothermal.

2. Reactor is isobaric, assuming pressure drop across the bed is significantly lower than the reactor pressure.
3. The gas is assumed to be of ideal behaviour. This is to allow the usage of ideal gas correlations in our simulation.
4. No internal mass transfer within the catalyst, mass transfer only occurs between bubble and emulsion phase.
5. No deactivation of catalyst.
6. Catalyst particles are suspended and there are no overall upward or downward flow with the exception of entrained particles arising from bursting bubbles.

4. Selection of Process Parameters

In this section, process parameters of the reactor will be examined. The chosen and optimized process parameters should obtain more than 800 kt/a plant capacity, while reducing the cost required to attain such specification. The process parameters will impact the reactor and auxiliary equipment designs, and thus affect the capital and operational expenditure of the section.

The process parameters being looked at in this section are catalyst, temperature, pressure, weighted hourly space velocity (WHSV), diameter as well as the height of the reactor.

4.1 Catalyst parameters

The particle properties of the catalysts were obtained similarly from the same study with some minor adjustments to achieve a more realistic simulation. The properties are as shown below:

Table 2: Catalyst properties

Parameter	Type/Value
Catalyst	Zeolite ZSM-5
Particle powder classification	Geldart A
Mean particle diameter, D_p (µm)	180
Fine fraction	0.004
Superficial velocity at minimum fluidization, U_{mf} (m/s)	0.0118
Particle density, ρ_s (kg/m^3)	1270
Pore size (Å)	5.8
Bed packing density at minimum fluidization, ρ_{mf} (kg/m^3)	744
Voidage at minimum fluidization, ε_{mf}	0.405

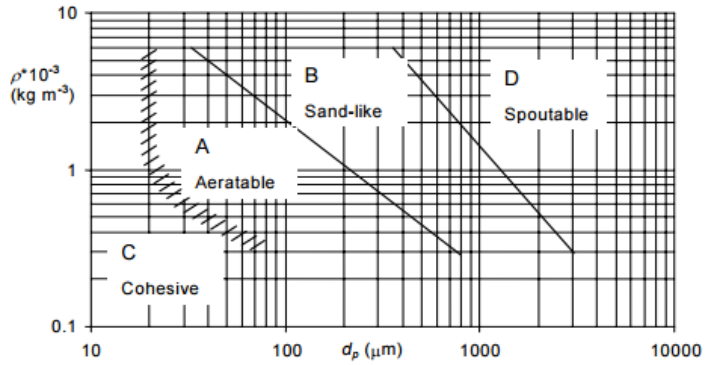

Figure 3: Geldart powder classification

The mean D_p was increased from the literature value of 108μm to 180 μm in order to increase the U_{mf}, and thus the design superficial velocity, U_0 required, while maintaining a Geldart type A particle regime that our hydrodynamic correlations discussed previously was based on.

In order to decide on an internal diameter of the reactor, the design U_0 of the feed flow would need to be approximated. U_{mf} was first calculated using the Wen and Yu (1965) correlation stated in the hydrodynamic correlation, and then a design U_0 was then approximated using the guideline of 8.5 times U_{mf} provided by Towler et al, (2013). By increasing the U_{mf} required via the increase in ZSM-5 particle size, D_p, and thus the design U_0, the internal diameter of the reactor could be reduced since its dependent on the design U_0 for a given fixed volumetric flow rate of gaseous feed. Figure 4 below shows the correlation between particle size and diameter of the reactor.

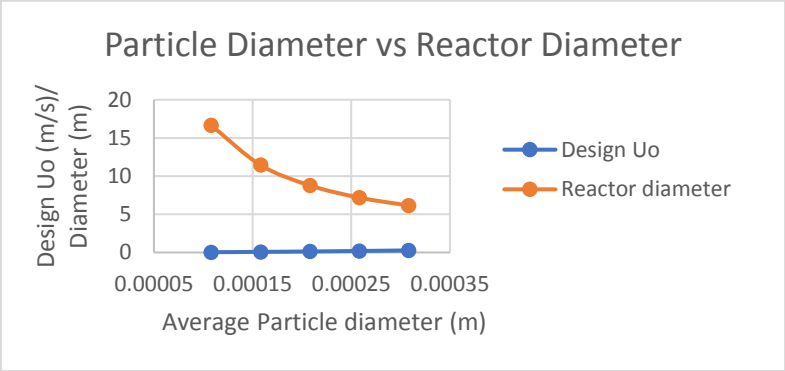

Figure 4: Correlation between mean particle size with design U_o and D_i

As can be seen, as the average D_p increased from 108μm to 308μm, the design superficial velocity increased from 0.03668 m/s to 0.2698 m/s. Since the volumetric flow rate was constant, this meant a reduction in the reactor cross sectional area required, and thus reducing the reactor diameter. As such, the average D_p was chosen to be increased to 180 μm.

4.2 Temperature

4.2.1 Temperature effects on olefin distribution

Temperatures between 450-550^{o}C were investigated, due to the model fitting with respect to main olefin species relatively well at this range of temperature (Kaarsholm et al., 2010), and temperatures outside this range could not be investigated without sacrificing much accuracy.

In order to keep other variables from affecting the simulation, the feed rate, amount of catalyst used, and operating pressure were kept constant. For our simulations, a WHSV of 15.67 h^{-1} with a methanol (99.6 wt % methanol, 0.4wt% water) feed flow rate of 3.73 kmol/s at 30 atm pressure were assumed.

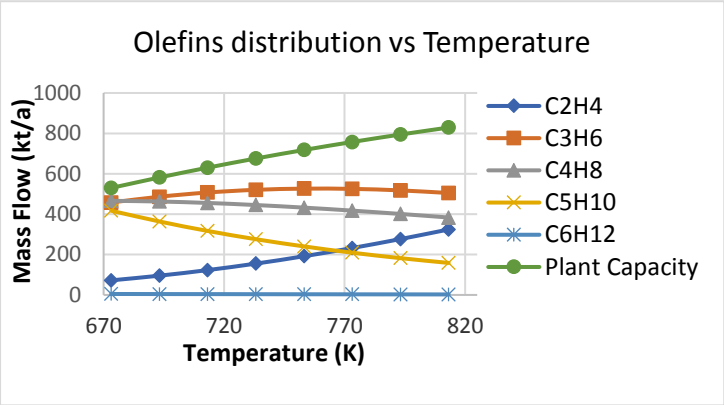

Figure 5: Olefins distribution vs temperature

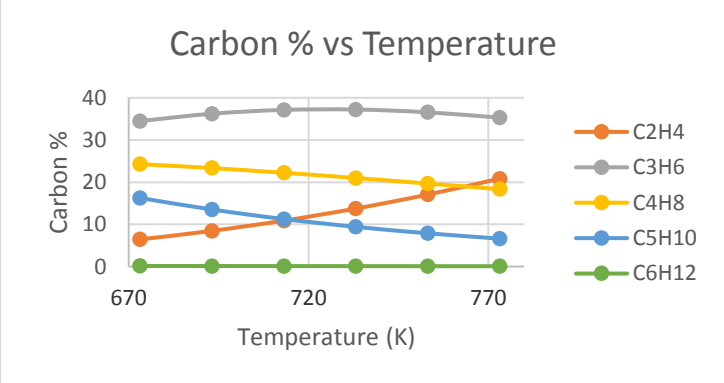

Figure 6: Olefins carbon % vs temperature

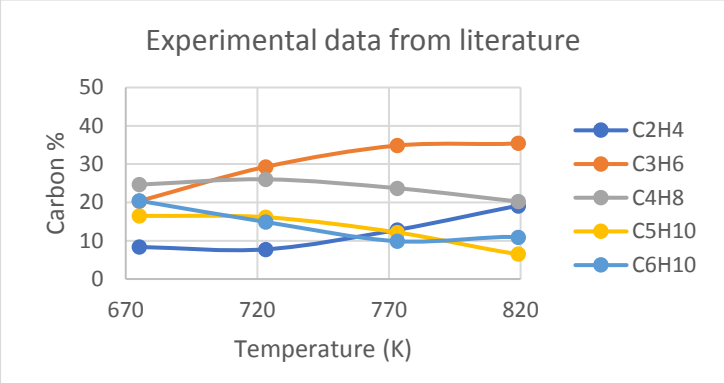

Figure 7: Olefins carbon % vs temperature from literature

As can be seen, the general trend of ethylene carbon % could be seen increasing along with the increase in temperature, while the heavier olefins (butane, pentene and hexene) were found to be decreasing with the increase in temperature. By comparing the trend of species distribution with that of the experimental data, the model was found to be largely congruent with the experimental data obtained from the literature, with higher temperatures resulting in an increase in the ethylene fractions and a decrease in the higher fractions. Additionally, we could also note that the plant capacity increases with temperature, with it hitting 800 kt/a past 800 K for the current simulation conditions.

However, it could be noted that the trend of propylene of the simulated

model deviates from that of the experimental data rather significantly, with it decreasing rather than continuously increasing according to the experimental data. The methanol conversion was found to decrease as well, though only slightly from 88.9% at 450^{o}C to 87.5% at 550^{o}C, although experimental data showed an increase in methanol conversion with increased temperature. For the species which we found the trends to correspond to that of the experimental data, their specific carbon % at each temperature point were found to differ slightly from that of the literature findings as well. These findings perhaps could be attributed to either inaccuracy of the model, or due to the difference in the operating pressure, WHSV, and feed composition utilized.

Additionally, it could be noted that the amount of C_6H_{12} produced in the simulation model, was significantly lower than that of experimental results. This disparity between the model and the experimental data had been acknowledged by Kaarsholm et al. in the same study, and it was explained to be perhaps due to the C_6H_{12} fraction in the model lumping both aromatics and large olefins, and these species would very likely require a separate kinetics due to differences in mechanism.

Overall, the model gave trends similar to that of the experimental data when temperature was varied, and could fit the data fairly well with the exception of propylene and hexene. However, a limitation to this investigation was that catalyst deactivation was not considered. The experiments performed by Kaarsholm et al., (2010) were conducted over a period of 4-5 hours, where the catalyst was still stable and the effects of reversible and irreversible deactivation of catalyst were negligible (Kaarsholm et al., 2010). As such, since the model was adapted to model after the experimental data, the model utilized would be incapable of investigating temperature's effect on deactivation, and hence its intricate effects on the product distribution.

4.2.2 Optimization of temperature

In order to determine the optimum temperature at which the reactor should be at, the optimum temperature should fulfil 2 criteria: 1) Maximizing profitability, which would be approximated by a preliminary estimation of the profit margin of the reactor section, and 2) Attaining a minimum plant capacity (ethylene and propylene) of 800 kt/a.

While generating more lighter olefins would generate more revenue, and it could be easily achieved by increasing the temperature as seen from the previous section, an increase in temperature would affect the cost of manufacture as well as the fixed capital investment.

In this section, for the sake of ease of optimization and the many temperature points, assumptions will be made and methodology used for the preliminary calculations of cost would be only briefly described, with the detailed calculations left out.

4.2.2.1 Estimating Operating Expenditure (OPEX)

In order to calculate the operating expenditure, the following methodology was utilized:

1. The reactor was simulated using MATLAB for temperatures between 450°C to 550°C, while fixing the feed flow rate at 3.73 kmol/s, pressure at 30 atm, and WHSV at 15.67 h^{-1} to obtain the flow rate and composition of product stream at each temperature point.
2. The feed pump, heater and the reactor were simulated with Aspen HYSYS by keying in the values obtained from MATLAB.
3. Feed heating duty and feed pump duty for each temperature point were then obtained from Aspen HYSYS. The feed heating duty was found to increase with temperature while feed pump duty remained the same.
4. The heating duty was assumed to be provided by a 100% thermal efficiency fired heater utilizing No. 2 Heating Oil, which has a heating duty of 9320 kcal/liter and a price of SG$ 0.986/liter.
5. The cost of feed heating duty was calculated for each temperature point.
6. The cost of feed pump duty was calculated for each temperature point using the electricity price of SG$ 6.222E-05/kJ.
7. The cost of feed heating duty and feed pump duty were assumed to be the only contributing component to utility cost, as cost of cooling the reactor was assumed to be provided by seawater and considered negligible.
8. Raw material cost, comprising of only methanol at the moment, was calculated using the price of SG$ 352.5/tonne.
9. The Operating Expenditure (OPEX) of the section was then assumed to consist of just the raw material cost and utility cost.

Table 3: Estimated OPEX with respect to temperature

Temperature (K)	Raw material cost (SG$/annum)	Utility cost (SG$/annum)	Estimated Operating Expenditure (SG$/annum)
723.15	1.326E+09	3.087E+08	1.635E+09

743.15	1.326E+09	3.132E+08	1.639E+09
763.15	1.326E+09	3.177E+08	1.644E+09
783.15	1.326E+09	3.223E+08	1.648E+09
803.15	1.326E+09	3.269E+08	1.653E+09
823.15	1.326E+09	3.316E+08	1.657E+09

As seen, as the temperature rises, the operating expenditure was found to be increasing. In addition, utility cost was found to be a small fraction of raw material cost, and contributed little to the operating expenditure.

4.2.2.2 Estimating Capital Expenditure (CAPEX)

In order to estimate our CAPEX, the following methodology was utilized:

1. From the MATLAB simulation performed at each temperature point, the reactor dimensions were obtained. Reactor diameter was designed to increase with temperature to accommodate the expansion in inlet gas volume to maintain the same design superficial velocity U_0, which is given by 8.5 times the U_{mf} as mentioned previously. The bed height decreases naturally as the reactor tube area increases due to the mass and packing density of the catalyst being the same.
2. Transport disengagement height (TDH) was calculated. Since the superficial velocity at the end of the bed was found to be approximately the same at 0.100 m/s throughout all the temperatures, the transport disengaging height is assumed to be the same, which was found to be 1.019 m.
3. The height of the reactor was calculated, which we assumed to be simply the sum of the bed height and the transport disengagement height.
4. The volume of the reactor was then calculated, and the module costing estimation proposed by Turton et al., (2016) was utilized to calculated the bare module cost of the reactor shell. Stainless steel grade 410 was assumed to be utilized for its high maximum temperature and corrosion resistance.
5. Module costing of furnace and pump was performed by assuming a non-reactive fired heater and a positive displacement pump.
6. The CAPEX was estimated, by assuming that the only contribution is from the bare module cost of the reactor shell, pump and furnace. CEPCI of 543 for year 2016 was considered. Cost for internals such as cooling coil, cyclone and distributor plate were

not considered as a change in design temperature does not change their costing that much, and cost of catalyst was not considered in this section as well due to the WHSV being kept constant.

The bare module cost, C_{BM}, and the estimated CAPEX of the reactor section at each temperature point are as shown in Table 6 below.

Table 4: Estimated CAPEX with respect to temperature

Temperature (K)	C_{BM} of Pump (SG$)	C_{BM} of Furnace (SG$)	C_{BM} of Reactor (SG$)	Total C_{BM} of Reactor Section (SG$)	FCI/ C_{TM} of Reactor Section (SG$)
723.15	1.160E+06	1.807E+07	1.304E+07	3.227E+07	3.807E+07
743.15	1.160E+06	1.844E+07	1.343E+07	3.303E+07	3.898E+07
763.15	1.160E+06	1.882E+07	1.382E+07	3.381E+07	3.989E+07
783.15	1.160E+06	1.921E+07	1.422E+07	3.459E+07	4.082E+07
803.15	1.160E+06	1.959E+07	1.462E+07	3.537E+07	4.174E+07
823.15	1.160E+06	1.998E+07	1.502E+07	3.617E+07	4.268E+07

4.2.2.3 Estimating profitability

For our calculations in this section, depreciation, and tax rate are assumed to be zero, and the rate of return is assumed to be 2.00%. Assuming a plant lifespan of 10 years, the annualized capital cost based on CAPEX could be obtained. Ethylene, propylene, and butylene are assumed to be to only source of revenue in our calculation of unit profit margin assuming 100% recovery. The prices of SG$ 1379/ tonne, SG$ 1226/ tonne, and SG$ 1677/ tonne for ethylene, propylene, and butylene were used. By subtracting the revenue with the total annualized cost obtained by adding annualized capital cost and OPEX, the net profit margin can be estimated.

Table 5: Profitability with respect to temperature

Temperature (K)	Annualized Capital Cost (SG$/annum)	Total Annualized Cost (SG$/ annum)	Revenue from C2, C3 and C4 (SG$/ annum)	Net profit margin (SG$/ annum)
723.15	4.239E+06	1.517E+09	1.578E+09	6.030E+07
743.15	4.339E+06	1.522E+09	1.617E+09	9.496E+07
763.15	4.441E+06	1.527E+09	1.650E+09	1.228E+08

783.15	4.544E+06	1.532E+09	1.677E+09	1.448E+08
803.15	4.647E+06	1.537E+09	1.699E+09	1.619E+08
823.15	4.751E+06	1.542E+09	1.717E+09	1.749E+08

As can be seen from the increase in profit margin, an increase in temperature was found to increase the plant capacity to the extent that even with the increased capital and operating expenditures, it is still more economically viable to run at a higher temperature compared to lower temperatures. As such, we have chosen our operating temperature to be at **550°C**.

4.3 Pressure

4.3.1 Pressure effects on olefin distribution

In our determination of how pressure affects light olefin distribution, we have decided to investigate pressures from 1 atm to 30 atm. We assume isobaric operation for our fluidized bed. A flow rate of 3.73 kmol/s at a WHSV of 15.67 h^{-1} was utilized in our investigation.

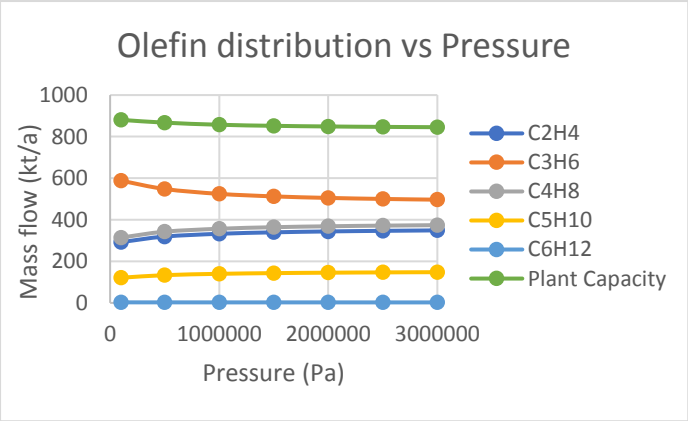

Figure 8: Olefins mass distribution with pressure

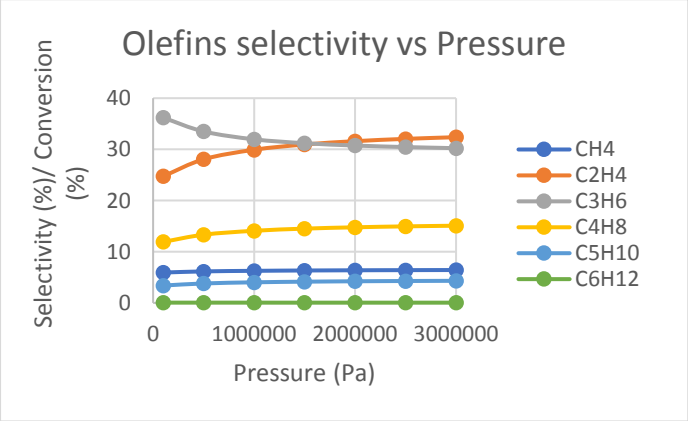

Figure 9: Olefins selectivity with pressure

As could be seen, as the pressure increases, the plant capacity decreases slightly from 880 to 846 kt/a. The methanol conversion was found to increase just a bit from 85.4% at 1 atm to 87.4% at 30 atm, indicating that pressure does not have a significant impact on conversion. The selectivity of propylene was found to decrease, but the selectivity of ethylene was found to increase instead with an increase in pressure. Pentene selectivity were found to increase as well, though only very slightly. These trends were found to be congruent with the study performed by Hajimirzaee et al., (2015) whose team investigated pressures from 1 bar to 20 bar.

However, the trend of the selectivity of butylene was found to differ from that of the study. In our investigations, butylene selectivity was found to increase with pressure, while in the study it was otherwise. Also, our trends of methane selectivity increased only slightly with the increase of pressure. However, in the literature, the increase was very sharp, and this massive increase was attributed to catalyst deactivation, which was not considered in our simplified model.

Apart from that, the general trends were similar to what was found in the literature, with the actual values of the selectivity differing just slightly likely due to a different feed composition, a different operating temperature of 400^{o}C and a different WHSV of 34 h-1 compared to ours.

4.3.2 Optimization of pressure

As can be seen from the previous section, an increase in pressure was found to reduce the plant capacity and light olefins conversion due to a reduction in propylene selectivity. In addition, an increase in pressure would incur additional utility costs in the form of pump duty. However, differences in pressure would result in a very different reactor design in terms of its dimensions, and as such a higher pressure might not necessarily mean lower profitability. Similar to temperature optimization, we would be looking at 1) profitability in terms of profit margin in reactor section and 2) maintaining a plant capacity of 800 kt/a, in our determination of an optimum pressure.

Similar as well, in this section, for the sake of ease of optimization and the many pressure points, assumptions will be made and methodology used for the preliminary calculations of cost would be only briefly described, with the detailed calculations left out.

4.3.2.1 Estimating Operating Expenditure (OPEX)

In order to calculate the operating expenditure with varying pressure, the following methodology was utilized:

1. The reactor was simulated using MATLAB for pressures between 1 atm to 30 atm, while fixing the feed flow rate at 3.73 kmol/s, temperature at 550^{o}C, and WHSV at 15.67 h^{-1} to obtain the flow rate and composition of product stream at each temperature point.
2. The feed pump, heater and the reactor were simulated with Aspen HYSYS by keying in the values obtained from MATLAB.

3. Feed heating duty and feed pump duty for each pressure point were then obtained from Aspen HYSYS. The feed heating duty was found to decrease with pressure while feed pump duty was found to increase.
4. The heating duty was assumed to be provided by a 100% thermal efficiency fired heater utilizing No. 2 Heating Oil, which has a heating duty of 9320 kcal/liter and a price of SG$ 0.986/liter.
5. The cost of feed heating duty was calculated for each pressure point.
6. The cost of feed pump duty was calculated for each pressure point using the electricity price of SG$ 6.222E-05/kJ.
7. The cost of feed heating duty and feed pump duty were assumed to be the only contributing component to utility cost, as cost of cooling the reactor was assumed to be provided by seawater and considered negligible.
8. Raw material cost, comprising of only methanol at the moment, was calculated using the price of SG$ 352.5/tonne.
9. The Operating Expenditure (OPEX) of the section was then assumed to consist of just the raw material cost and utility cost.

Table 6: Estimated OPEX with respect to pressure

Pressure (Pa)	Raw Material Cost (SG$/annum)	Utility Costs (SG$/annum)	Estimated Operating Expenditure (SG$/annum)
100000	1.326E+09	2.222E+08	1.548E+09
500000	1.326E+09	2.220E+08	1.548E+09
1000000	1.326E+09	2.001E+08	1.526E+09
1500000	1.326E+09	1.998E+08	1.526E+09
2000000	1.326E+09	1.995E+08	1.525E+09
2500000	1.326E+09	1.991E+08	1.525E+09
3000000	1.326E+09	1.987E+08	1.525E+09

As can be seen, contrary to what was initially presumed, an increase in pressure actually decreased the amount spend on utility, and as such a decrease in the operating expenditure. This was because the heat duty required at higher pressures and the cost associated were way lower compared to the increased pump duty and its operating cost.

4.3.2.2 Estimating Capital Expenditure (CAPEX)

In order to estimate our CAPEX, the following methodology was utilized:

1. From the MATLAB simulation performed at each pressure point, the reactor dimensions were obtained. Reactor diameter was designed to decrease with increasing pressure to accommodate the expansion in inlet gas volume to maintain the same design superficial velocity U_0, which is given by 8.5 times the U_{mf} as mentioned previously. The bed height decreases naturally as the reactor tube area increases due to the mass and packing density of the catalyst being the same.
2. Transport disengagement height (TDH) was calculated. Since the superficial velocity at the end of the bed was found to be approximately the same at 0.100 m/s throughout all the temperatures, the transport disengaging height is assumed to be the same, which was found to be 1.019 m.
3. The height of the reactor was calculated, which we assumed to be simply the sum of the bed height and the transport disengagement height.
4. The volume of the reactor was then calculated. At 1 atm, reactor volume is found to be huge at 2639 m^3 compared to 123.7 m^3 at 30 atm due to the huge reactor diameter.
5. The module costing estimation proposed by Turton et al, was utilized to calculated the bare module cost of the reactor shell. Stainless steel grade 410 was assumed to be utilized for its high maximum temperature and corrosion resistance.
6. Module costing of furnace and pump was performed by assuming a non-reactive fired heater and a positive displacement pump.
7. The CAPEX was estimated, by assuming that the only contribution is from the bare module cost of the reactor shell, pump and furnace. CEPCI of 543 for year 2016 was considered. Cost for internals such as cooling coil, cyclone and distributor plate were not considered as a change in design temperature does not change their costing that much, and cost of catalyst was not considered in this section as well due to the WHSV being kept constant.

The bare module cost and the estimated CAPEX of the reactor section at each pressure point are as shown in Table 9 below.

Table 7: Estimated CAPEX with respect to pressure

Pressure (Pa)	C_{BM} of Pump (SG$)	C_{BM} of Furnace (SG$)	C_{BM} of Reactor (SG$)	Total C_{BM} of Reactor Section (SG$)	FCI/ C_{TM} of Reactor Section (SG$)

100000	0.000E+00	2.092E+07	1.164E+08	1.373E+08	1.620E+08
500000	2.644E+05	2.089E+07	3.265E+07	5.381E+07	6.349E+07
1000000	3.673E+05	1.915E+07	2.177E+07	4.129E+07	4.872E+07
1500000	5.653E+05	1.912E+07	1.842E+07	3.810E+07	4.496E+07
2000000	7.632E+05	1.907E+07	1.682E+07	3.665E+07	4.325E+07
2500000	9.612E+05	1.903E+07	1.592E+07	3.591E+07	4.238E+07
3000000	1.159E+06	1.898E+07	1.539E+07	3.554E+07	4.193E+07

4.3.2.3 Estimating profitability

Similar to temperature optimization with the same assumptions and prices, the total annualized capital cost and net profit margin of reactor section for each operating pressure could be obtained as follows:

Table 8: Profitability with respect to pressure

Pressure (Pa)	Annualized Capital Cost (SG$/annum)	Total Annualized Cost (SG$/annum)	Revenue from C2, C3 and C4 (SG$/ annum)	Net profit margin (SG$/ annum)
100000	1.804E+07	1.566E+09	1.650E+09	8.432E+07
500000	7.069E+06	1.555E+09	1.686E+09	1.312E+08
1000000	5.424E+06	1.531E+09	1.699E+09	1.681E+08
1500000	5.005E+06	1.531E+09	1.707E+09	1.761E+08
2000000	4.815E+06	1.530E+09	1.711E+09	1.813E+08
2500000	4.718E+06	1.530E+09	1.715E+09	1.849E+08
3000000	4.668E+06	1.529E+09	1.717E+09	1.876E+08

As can be seen, the profit margin of the reactor section with increasing pressure. Revenue from light olefins and butene were found be increasing with pressure due to the higher selectivity of butene generating additional revenue, despite a decrease in plant capacity (C2 and C3 fractions). As such, our optimum pressure was chosen to be at **30 atm**.

4.4 WHSV

4.4.1 Effect of WHSV on olefin distribution

By utilizing the optimized temperature and pressure of 550 ^{o}C and 30 atm respectively, the relationship between WHSV and olefin distribution was investigated. To do so, we kept the feed flow rate at 3.73 kmol/s, and increased the amount of catalyst used to vary the WHSV.

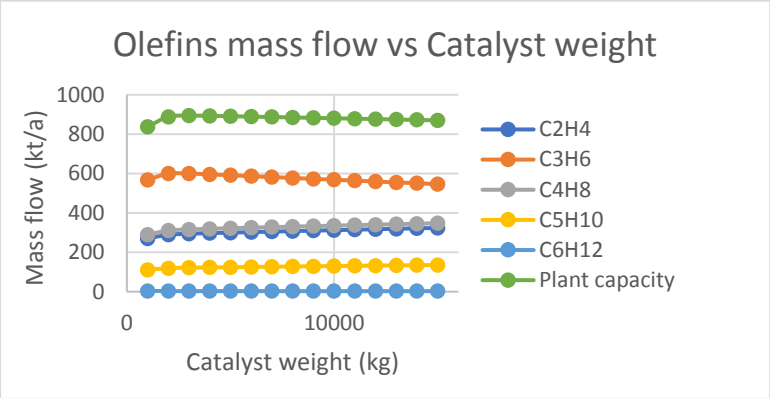

Figure 10: Olefins mass distribution with catalyst weight

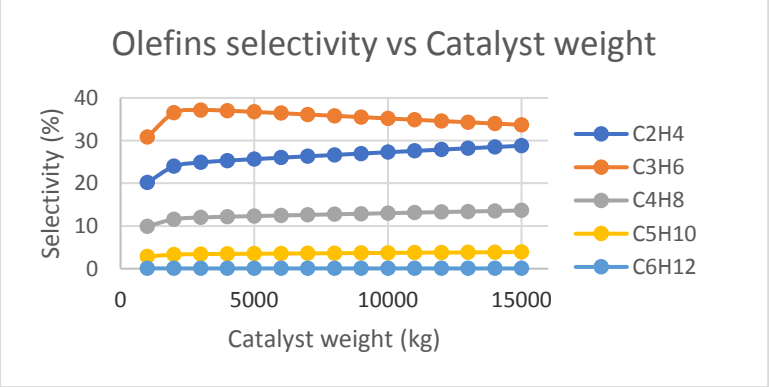

Figure 11: Olefins selectivity with catalyst weight

As the WHSV decreases (increasing catalyst weight) from 431 h^{-1} to 28 h^{-1}, conversion of methanol was found to be increasing from 79.3% to 86.5%. Selectivity of propylene was found to increase at first to a maximum of 37% at 143 h^{-1}, but decreases gradually after which as contact time increases. Ethylene selectivity was found to increase slightly from 20.3% to 28.9% in this range as well. These observations were found to be congruent with that the study conducted by Hajimirzaee et al., (2015) with slight differences in the actual numbers.

However, while the study found that higher olefins, such as butylene and pentene, decreased with decreasing WHSV, we found them to increase instead. Butylene was found to increase from 9.95% to 13.6% slightly over the range between 431 h^{-1} to 28 h^{-1}, and pentene was found to increase slightly as well. Hexene was found to be decreasing, similar to the trend of the literature however. The experimental data obtained by Kaarsholm et al. (2010) revealed that butylene and pentene carbon % did not show a clear trend when measured at 550 ^{o}C with residence time between 2.5-5.5 seconds. As such, this could be one of the reasons to the inaccuracy in trend predicted by our model.

In addition, the methanol conversion was found to be rather low compared to that of experimental results by Kaarsholm et al. Experimental results showed that conversion had reached close to 100% after a residence time of 4 seconds at 550^{o}C, while simulations utilizing the model had a mere 85.2% conversion after a contact time of 25 seconds at 550^{o}C and 30 atm operating conditions. This disparity could be attributed perhaps to the difference in pressure, as an operating pressure was not mentioned in the literature, or could be attributed to the differences in inlet flow rate.

The plant capacity was found to first increase sharply with decreasing WHSV initially, and then decreases as contact time was increased. This finding was congruent to study by Hajimirzaee et al., who found out that by increasing WHSV, light olefins are more favoured due to there being not enough time for light olefins to form paraffins and aromatics due to the hydrocarbon pool mechanism (Hajimirzaee et al., 2015). The plant capacity was found to be at its maximum at 893.6 kt/a at WHSV of 134 h^{-1}, which corresponds to approximately 3200 kg of ZSM-5 catalyst being used with the operating conditions the simulation used.

4.4.2 Optimization of WHSV

As seen from the previous section, a higher WHSV of 134 h^{-1} was actually beneficial in the production of lighter olefins, as lighter olefins were found to decrease with increasing contact time. In addition, a higher WHSV would mean a lesser amount of catalyst used, which would mean a reduction in capital expenditure as well, however small.

While there was found to be an increase in butylene according to our model as contact time increases, and as such would lead to a slight increase in revenue, it was likely to be not accurate due to the reasons mentioned in the previous section. With that in mind, we have decided that the optimum WHSV to use for our reactor to be **134 h^{-1}**.

4.5 Feed rate

When choosing a feed rate, it should be enough such that there is at least approximately 880 kt/a of light olefins being produced. The additional 80 kt/a from the 800 kt/a plant capacity specification is to compensate for losses that might occur during downstream separation and purification processes. In order to increase light olefins production and methanol conversion, we have incorporated a recycle stream which feeds methanol and dimethyl ether from the reactor outlet back into the reactor inlet stream. By running the simulation using our optimized parameters, in order to obtain an 882 kt/a plant capacity, the feed rate required was found to be **3161 kt/a** assuming an 8000-hour work year.

4.6 Reactor Diameter

As mentioned in the catalyst parameters section, the reactor diameter is dependent on the feed volumetric flow rate and U_{mf}. In order to decide on the reactor diameter, the following methodology was used in our MATLAB simulation.

1. Minimum fluidization velocity was determined using to be 0.0118 m/s using the Wen and Yu (1965) correlation as shown below:

$$\mathbf{u}_{mf} = \frac{\mu}{d_p \rho_g}\left[\left[(33.7)^2 + 0.0408\left(\frac{d_p^{\,3}\rho_g(\rho_s - \rho_g)g}{\mu^2}\right)\right]^{1/2} - 33.7\right]$$

   where μ is gas viscosity, ρ_g is gas viscosity and g is the gravity constant.
2. A design superficial velocity was set at 8.5 times U_{mf}, which is 0.100 m/s, to ensure adequate turndown and prevent excessive entrainment of catalyst particles according to guidelines by Towler et al., (2013).
3. The set design superficial velocity, U_0, was then checked against the terminal velocity of the particles, U_t, (ie. Maximum fluidization velocity) to ensure that the superficial velocity is not higher than the terminal velocity. The terminal velocity of the catalyst particle was determined to be 0.370 m/s using the correlation given by Kunii and Levenspiel (1997) below:

$$u_t = \left(1.78 \times 10^{-2}\, \eta^2/\rho_g \mu\right)^{1/3}\left(d_p\right)$$

   where η is the gravitation term given by $g(\rho_s - \rho_g)$.
4. Feed volumetric flow rate was found, using the molar flow rate required to hit plant specification, assuming an ideal gas correlation. Subsequently, the area and the diameter of the reactor can be found using the following correlations:

$$feed\ volumetric\ flow\ rate = area\ of\ reactor \times design\ superficial\ velocity$$

$$area = \pi \times diameter^2/4$$

As such, the reactor diameter was found to be **9.915m**.

4.7 Reactor Height

In order to calculate the reactor height required, the following methodology was used in our MATLAB simulation.

1. Expanded volume of bed was first determined using the bed density at minimum fluidization and the mass of catalyst required in the bed.
2. From the expanded volume of bed and the already determined reactor diameter, the bed height at minimum fluidization could be calculated, which was found to be 0.0513 m.

The bed height when bubbling fluidization occurs was assumed to be the same as that at minimum fluidization, and that splashing does not affect the bed height. This bed height was also assumed to be the maximum.

3. The bed height, H_{mf}, was then checked to ensure that slugging would not occur using the correlation below:

$$\left(\frac{H_{mf}}{D}\right) \leq \frac{1.9}{(\rho_p x_p)^{0.3}}$$

where ρ_p is catalyst density, D is the reactor internal diameter and x_p is mean particle diameter.

4. In order to account for disengagement of catalyst particles due to bursting bubbles, the Transport Disengagement Height (TDH) was calculated to be 1.074 m using the following correlation proposed by Fournol et al (1973):

$$TDH(F) = 1000\,\frac{U^2}{g}$$

where U is the superficial velocity, and g is the gravity constant.

5. Additional allowance to the height was added to make space for cyclones and feed distributor.

By adding the TDH with the bed height, the height of the reactor was found to be **1.125 m**. This height is tentative however, and would be further lengthened to make allowance for the internals such as cyclones and feed distributor subsequently.

4.8 Optimized parameters

Table 11 below summarizes the process conditions and reactor dimensions that were optimized for the methanol to olefin process.

Table 9: Optimized reactor parameters

Parameter	Value
Reactor Internal Diameter (m)	9.915
TDH (m)	1.074
Bed Height at minimum fluidization (cm)	5.13
Methanol Feed Rate (kt/a)	3161
WHSV (h^{-1})	134
Mass of Catalyst used (kg)	2949
Operating Pressure (atm)	30

Operating Temperature (°C)	550
Plant Capacity (kt/a)	882.6

As mentioned in previous sections, these conditions were chosen based on weighing profit to expenses, and to maintain a plant capacity of at least 880 kt/a. Using these parameters, these two criteria were met.

5. Section Configurations and Equipment Design Considerations

With the process parameters optimized and dimensions of the reactor settled, herein discusses the choices made to configuration of the reactor section and considerations with regards to the design of the equipment utilized in the section. Choices here would affect capital expenditure (CAPEX) and operating expenditure (OPEX) of the section as well.

5.1 Recycle

As mentioned previously, in order to improve the plant capacity, all of the methanol and dimethyl ether from the reactor outlet stream were recycled back to the reactor for further reaction. The setup is as shown below:

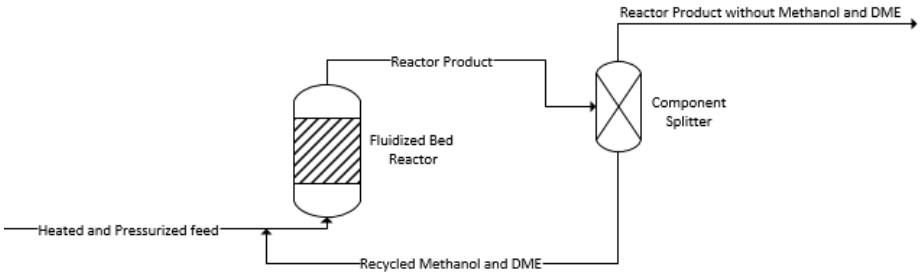

Figure 12: PFD of recycle section

The component splitter illustrated in the diagram above is representative of all the purification and separation processes required to separate a pure stream of methanol and dimethyl ether from the reactor outlet stream. Realistically, the series of separation processes required for this to occur would incur much cost and design considerations. However, for the sake of simplification, the costing and design of these separation processes were assumed to be negligible in the final calculation of section costing that would be done in a later section.

Using the same operating parameters and the same reactor dimensions, a methanol conversion of **98.2%** and a plant capacity of **882.6 kt/a** were attained. This is in contrast with the 85.2%

methanol conversion and a plant capacity of 739.5 kt/a obtained without the recycle stream. As such, the recycle was found to be effective in improving light olefins production and methanol conversion.

5.2 Heating of feed and cooling of reactor

In order to heat the feed up from 25ºC to 550ºC, a series of 3 fired heaters would be used. The first one is to heat the feed from 25ºC to 172ºC, the boiling point of the feed mixture, the second would be to boil the feed, and the last one to heat the vapor from 172.2ºC to 550ºC. Using Aspen HYSYS, the respective heat duties are found to be as follows: **64300 kW, 72300 kW and 104300 kW**. The fuel used was decided to be **natural gas**.

In order to keep our fluidized bed reactor isothermal, it is necessary for it to be cooled since the reactions are exothermic. As proposed by Towler et al., (2013), one way is to use a cooling coil within the fluidized bed reactor, and another way is to utilize a cooling jacket surround the reactor to cool the contents within. The cooling duty required, Q, was found using Aspen HYSYS to be **127300kW**, and due to the high duty required a higher heat transfer surface area provided by the coil would be more suitable. The overall heat transfer coefficient, U, estimated by Towler et al., for immersed cooling coil is 500- 1000 W/m^2.K assuming steam is used. For our design, a moderately conservative estimate of **750 W/m^2.K** was used.

$$A = \frac{Q}{U\Delta T_m} = \frac{127300\times1000}{750\times\frac{525-350}{\ln(^{525}/_{350})}} = 393.3\ m^2$$

where A is the heat transfer area and ΔT_m is the mean temperature difference between the two streams. Using the above equation, assuming 25ºC water was used for inlet of coil and exits the coil at 200 ºC as superheated steam while keeping the reactor isothermal at 550ºC, the surface area required was found to be **393.3 m^2**.

The mass flow of water required was calculated to be **1506 kt/a** using the following equation.

$$Mass\ flow\ of\ steam = \frac{Q}{\Delta H_{water}} = \frac{127300}{2700-267} = 52.3\ kg/s = 1506\ kt/a$$

where ΔH_{water} is change in enthalpy of water. The cost of cooling water was considered to be negligible.

Since the coil will be immersed in the fluidized bed, the same material would be used for the construction of coils as the reactor shell.

5.3 Pump

In order to obtain the required pressure of 30atm, a pump to pressurize the feed is required. To prevent the usage of a compressor, which is more expensive compared to a pump, the feed was pressured first before being heated and converted into vapor. To size the pump, the steps used are detailed below:

1) Obtain volumetric flow rate and density of methanol feed from Aspen HYSYS.
2) Obtain pressure difference between inlet and outlet of the positive displacement pump using Aspen HYSYS. The pressure drop is assumed to be negligible.
3) Pump head, H, is then calculated in meters. By using the following formula.

$$H = \frac{\Delta P}{\rho_R} \times 1.2 = \frac{2938000}{7717} = 456.8\, m$$

where ΔP is the pressure across pump in Pa and ρ_R is the density of feed stream in N/m^3. An oversize factor of 1.2 is applied for a more conservative estimation in the determination of pump head.

Using the above methodology, the pump head was found to be **456.8 m**. The pump duty required was found to be **656.4 kW** using Aspen HYSYS assuming a **75% adiabatic efficiency**.

Since our pressure is high and would fluctuate as we would discuss in the section of catalyst regeneration, **a positive displacement pump** will be used for its versatility in variations of pressure and in high pressures (Pumpschool, 2007). **Stainless steel grade 410** will be used since methanol with water can be corrosive.

5.4 Catalyst regeneration and coke removal

While the simulation model did not take into account catalyst deactivation, catalyst regeneration is required due to the coke produced being deposited on the ZSM-5 catalyst reducing the catalyst's activity.

In order to regenerate our catalyst, there are two ways of doing it. Either continuous regeneration or batch wise regeneration. In order to ensure optimum uptime of the plant, we have decided to utilize continuous regeneration for our reactor.

One traditional way is to separate our catalyst out into a regenerator for regeneration by passing air to combust the coke, and return the catalyst back into our reactor. However, a limitation to

this is that the regeneration must be conducted in the absence of our organic reactants, and must be performed in another zone separate from where the methanol to olefins reactions are taking place. As such, this would incur additional capital costs in designing and purchasing a regenerator column. In addition, the burning of coke produces water, which at high temperatures can destroy the structure of the zeolite catalyst (Forbus et al., 1988).

In our design, we have decided to go with hydrogen treatment in our regeneration of catalyst. In the patent discussed by Forbus et al., (1988) indicated the benefits and guidelines of utilizing hydrogen treatment for regeneration. Using this regeneration method, zeolite based catalyst such as ZSM-5 can be regenerated even in the presence of organic reactants within the bubbling fluidized reaction zone, negating the need for regeneration in an external equipment. This can be done so by flowing hydrogen gas through the bubbling fluidized bed.

Recommended temperature for the regeneration process to occur ranges from 200^{o}C to 600^{o}C, and recommended pressure ranges from about 3 atm to 48 atm. As such, our optimized operating conditions of 550^{o}C and 30atm are well within the recommended ranges.

In order to perform further regeneration in case when the catalyst deactivates even while hydrogen is flowing, it is generally necessary to contact the catalyst with hydrogen at an elevated pressure above that of normal methanol to olefin conversion conditions. As such, it is necessary to perform scheduled checks on the catalyst, and increase the pressure as and when required. Unfortunately, due to an absence of kinetics, the effect of hydrogen on olefins distribution and the additional pressure and scheduling required could not be investigated and simulated. Thus, we have decided to use a conservative estimate of **35 atm as our elevated pressure** required to prevent too much deviation from our optimized parameters and design.

It was recommended by Forbus et al, that the molar ratio of hydrogen to organic reactants be 0.5:1 to 40:1. We have decided to use a conservative estimate of 0.5:1 molar ratio for now to prevent too much deviation from our optimized parameters and design due to the increased inlet volumetric flow rate. As such, by the mass flow rate of H2 required was found to be **98.47 kt/a** assuming 8000 hours operating year.

The coke and carbon formed from the MTO reaction are assumed to be removed completely by this regeneration process.

5.5 Cyclone

In order to remove the fine catalyst particles that are entrained in the gaseous product flow as a result of bubbles bursting, we would implement a cyclone with the inlet at the TDH. To size the cyclone, the following methodology proposed by Towler et al., (2013) was utilized:

1. Determine if the cyclone should be high efficiency or high throughput. Since our fine particles above TDH are less than 0.4%, a high throughput design will be utilized.
2. Using figure 10.44b in Towler's book, the cyclone diameter required for an inlet velocity of 15 m/s, D_c, was calculated to be 1.370 m for a volumetric flow rate of 7.925 m^3/s of the fluidized bed product flow.
3. Since D_c was too high compared to the standard design diameter of 0.203 m, we assume to use **8 cyclones in parallel**. The volumetric flow rate, Q, was calculated again to be 0.990 m^3/s for each cyclone. The D_c was calculated again to be **0.484 m**.
4. The difference in density between solids and liquid, ρ, was assumed to be the particle density of ZSM-5, which is 1270 kg/m^3, and the viscosity of the gaseous product flow, μ, was found to be 0.0255 cp using MATLAB simulation.
5. The scaling factor was calculated to be **2.385** using the following equation.

$$Scaling\ factor = \left[\left(\frac{Dc}{0.203}\right)^3 \times \frac{669}{Q} \times \frac{2000}{\rho} \times \frac{\mu}{0.018}\right]^{0.5}$$

6. The dimensions of one cyclone was then calculated using Figure 10.45b of Towler's book, utilizing the scaling factor and required cyclone diameter, D_c, calculated.

Figure 13 below shows the proposed design of 1 cyclone using the methodology mentioned above.

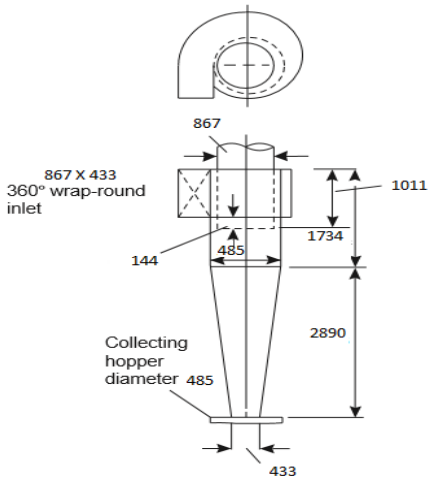

Figure 13: Dimensions of the sized cyclone

Volume of the cyclone was approximated with the shape of a cylinder, and was found to be **6.835 m^3**. The 8 cyclones in parallel would be placed above the TDH within the reactor.

5.6 Porous plate distributor

In order to distribute the gas flow evenly and to allow a stable bubbling fluidized bed operation, a porous plate distributor is needed. To design the porous plate distributor, the following methodology proposed by Kunii and Levenspiel (1997) was utilized.

1. Determine c, the ratio of pressure drop across orifice/ pressure drop across bed using the correlation below:

$$c = \exp\left(-3.8\times\frac{H_{mf}}{reactor\ diameter}\right) = \exp\left(-3.8\times\frac{0.0513}{9.915}\right) = 0.981$$

   where H_{mf} is bed height at minimum fluidization.

2. Calculate pressure drop across bed, Δp_B, using the correlation below:

$$\Delta p_B = \rho_p \times(1-\varepsilon_{mf})\times H_{mf}\times g = 1270\times 0.595\times 0.0513\times 9.81 = 380.2\ Pa$$

   where ρ_p is particle density, g is gravity constant and ε_{mf} is voidage at minimum fluidization.

3. Obtain Δp_d, the pressure drop across the distributor using c and pressure drop across bed. Found to be 372.9 Pa.

4. Since Reynolds number was found to be >3000, the orifice coefficient, $C_{d,or}$ was chosen to be 0.60.

5. The gas velocity through the orifice, u_{or}, was then calculated using the correlation below:

$$u_{or} = C_{d,or}\left(\frac{2\Delta p_d}{\rho_g}\right)^{1/2} = 0.60\left(\frac{2\times 372.9}{15.44}\right)^{1/2} = 4.169\ m/s$$

   where ρ_g is the inlet feed gas density.

6. The number of orifices per unit area of distributor, $\mathbf{N}_{or}$, was then decided to be **1000 orifices/m^2**. Subsequently, the corresponding orifice diameter, d_{or}, was calculated as shown below:

$$d_{or} = \left(\frac{4u_o}{\pi \boldsymbol{N}_{or} u_{or}}\right)^{1/2} = \frac{4\times 0.1}{3.142\times 1000\times 4.169} = 0.005525\ m$$

   where u_o is superficial velocity of feed.

From the above procedure, our orifice diameter was found to be **5.525 mm**, and the number of orifices on the distributor was found to be **77220 orifices**. The porous plate distributor would be made of the same material as that of the reactor shell. Due to there being no correlations for estimating distributor cost, we assume the cost to be **negligible**.

The height of the windbox was decided to be **10 cm**.

5.7 Reactor shell

Factoring in the considerations of our reactor internals by adding the heights of the bed, cyclones, TDH and windbox, the new reactor height was calculated to be **5.849 m**. reactor diameter remains at **9.915 m**.

The choice of material for the reactor was chosen to be **stainless steel grade 410**. This is because methanol with water can be corrosive, and that stainless steel is strong enough to withstand the high operating temperature of 550^{o}C.

Under Section VIII of the ASME Boiler and Pressure Vessel Code, the minimum thickness required for a cylindrical vessel wall to resist the internal pressure is given by:

$$t = \frac{P_i D_i}{2SE - 1.2P_i} = \frac{3800000 \times 9.915}{2 \times 84805515 \times 1 - 1.2 \times 3800000} = 0.228\ m$$

Where P_i is the design pressure, D_i is the internal diameter of the vessel, S is the maximum design stress found to be 84805515 Pa and E is the joint weld factor. The design pressure P_i was taken to be 10% above our normal operating pressure of 30-35 atm, and as such was chosen to be **38 atm**. The calculated minimum thickness for our fluidized bed reactor was found to be 22.8 cm due to the high design pressure. Factoring in additional 4 mm for corrosion allowance, the minimum thickness was decided to be **23.0 cm**.

5.8 Storage tank for methanol feed

Assuming shipment of methanol feed arrives once **every 3 hours** during operation, the storage tank should hold enough methanol feed for 3 hours of straight operation, which is found to be 1.185 kiloton. The storage tank was decided to be kept at ambient conditions of **25 ^{o}C and 1 atm**, and thus the feed would be in liquid phase. As such, the volume occupied by the liquid methanol feed was found to be 1482 m^3. To account for expansion, the volume of our storage tank was decided to be **1550 m^3**.

The material used was decided to be **stainless steel Grade 410** as methanol with water can be corrosive. Since methanol when mixed with water can be flammable, a **closed tank with a floating roof** will be used.

6. Cost Estimation of the Reactor Section

Turton et al., (2016) proposed bare module cost estimation of equipment using characteristic size factors as shown below:

$$C_{BM} = C_p^{\circ}(B_1 + B_2 F_M F_P)$$

$$log_{10} C_p^{o} = K_1 + K_2 log_{10}(S) + K_3 [log_{10}(S)]^2$$

Where F_P is obtained with equation A.2, F_M is obtained from Table A.3, B_1 and B_2 is given in Table A.4, K_1, K_2 and K_3 are obtained from tables A.1 of Turton's book. S is the size factor of the equipment in question. These would be utilized to estimate the total capital expenditure required for this section. The tabulated bare module cost, C_{BM}, in SG$ in 2016 (CEPCI = 543), of the reactor and other equipment of the section are as shown in Table 12.

Table 10: CAPEX of reactor section

Cost of Reactor (CRV-101)			
Reactor Shell		**Internal Coil**	
Volume	451.7 m^3	Surface Area	426 m^2
C_{BM}	**$4.922E+07**	U	750 $W/m^2.K$
Cyclones		**C_{BM}**	**$2.250E+06**
Volume of 8 Cyclones	6.835 m^3		
C_{BM} of 8 Cyclones	**$6.579E+04**		
C_{BM} of Reactor		**$5.153E+07**	
Cost of Auxiliary Equipment			
Fired Heater 1 (E-101)		**Positive Displacement Pump (P-101)**	
Duty	64300 kW	Duty	656.4 kW
C_{BM}	**$5.168E+06**	Head	456.8 m
Fired Heater 2 (E-102)		**C_{BM}**	**$1.301E+06**
Duty	72300 kW	**Storage Tank**	
C_{BM}	**$5.672E+06**	Volume	1550 m^3
Fired Heater 3 (E-103)		**C_{BM}**	**$4.002E+05**
Duty	104300 kW		
C_{BM}	**$7.706E+06**		
Fixed Capital Investment of the Section			
Total Bare Module Cost, $\sum_i C_{BM,i}$		$7.178E+07	
FCI/ Total Module Cost, C_{TM}		**$8.470E+07**	

As seen, the total capital expenditure required was found to be **$8.470E+07** according to the price for May 2016 in Singapore Dollars. To compare the CAPEX with OPEX, the CAPEX calculated would have to annualized. This can be done by utilizing an expected rate of return for capital investment, and using the following equation:

$$Annualized\ Capital\ Cost\ = \ Capital\ Cost \times \frac{i(1+i)^{10}}{(1+i)^{10}-1} = 8.470E+07 \times \frac{0.02(1+0.02)^{10}}{(1+0.02)^{10}-1}$$

$$= \$9.429E+06$$

where i is the rate of return. The rate of return was assumed to be 2.00 % as a benchmark from US Treasury, and annualized over 10 years. The tabulated annualized capital cost amounts to **$9.429E+06** in May 2016 Singapore Dollars. The OPEX is summary of raw material and utilities needed from the plant, and is tabulated in Table 13 below.

Table 11: OPEX of reactor section

Utility Cost, C_{UT}			
Utility	**Quantity Required**	**Cost**	**OPEX/year in SGD**
Electricity	656.4 kW	6.222E-05 SG$/kJ	$1.176E+06
Natural Gas	240900 kW	2.6 US$/MMBTU	$2.411E+07
Hydrogen	98.47 kiloton/annum	1SG$/kg	$9.847E+07
Raw Material Cost, C_{RM}			
Raw Material	**Quantity Required**	**Cost**	**OPEX/year in SGD**
Methanol Feed	3161 kiloton/annum	352.5 US$/ton	$1.114E+09
Total OPEX/ year			
$1.238E+09			

7. Process Flow Diagram

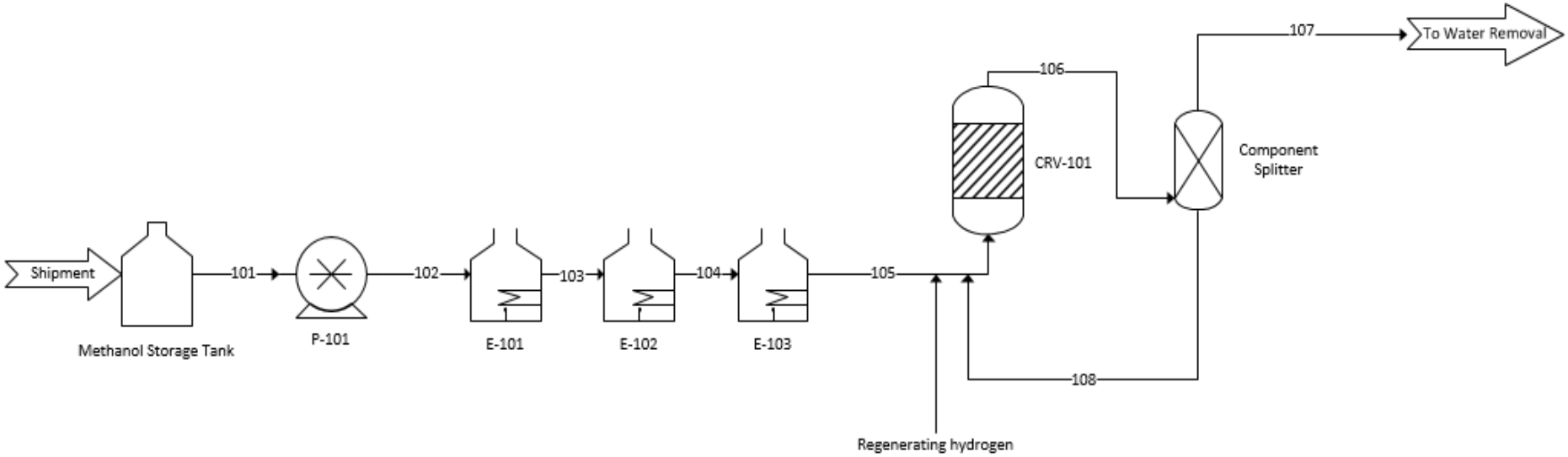

8. Stream Data

Stream Number	101	102	103	104	105	106	107	108	Hydrogen
Vapour Fraction	0.00	0.00	0.00	1.00	1.00	1.00	1.00	1.00	1.00
Temperature (°C)	2.50E+01	2.67E+01	1.72E+02	1.72E+02	5.50E+02	5.48E+02	5.50E+02	4.67E+02	5.50E+02
Pressure (kPa)	1.01E+02	3.65E+03	3.04E+03	3.04E+03	3.04E+03	3.04E+03	3.04E+03	3.04E+03	3.04E+03
Molar Flow (kgmole/h)	1.23E+04	1.23E+04	1.23E+04	1.23E+04	1.23E+04	2.27E+04	2.25E+04	2.65E+02	5.58E+03
Mass Flow (kg/h)	3.93E+05	3.93E+05	3.93E+05	3.93E+05	3.93E+05	4.17E+05	4.08E+05	9.02E+03	1.12E+04
Liquid Volume Flow (m^3/h)	4.94E+02	4.94E+02	4.94E+02	4.94E+02	4.94E+02	7.47E+02	7.36E+02	1.17E+01	1.61E+02

Heat Flow (kJ/h)	-2.95E+09	-2.95E+09	-2.72E+09	-2.46E+09	-2.08E+09	-2.46E+09	-2.41E+09	-4.53E+07	8.56E+07
Component	**Mole Fraction**								
Water	0.0071	0.0071	0.0071	0.0071	0.0071	0.5509	0.5574	0.0000	0.0000
Methanol	0.9929	0.9929	0.9929	0.9929	0.9929	0.0100	0.0000	0.8581	0.0000
diM-Ether	0.0000	0.0000	0.0000	0.0000	0.0000	0.0017	0.0000	0.1419	0.0000
Ethylene	0.0000	0.0000	0.0000	0.0000	0.0000	0.0565	0.0572	0.0000	0.0000
Propylene	0.0000	0.0000	0.0000	0.0000	0.0000	0.0777	0.0786	0.0000	0.0000
1-Butene	0.0000	0.0000	0.0000	0.0000	0.0000	0.0304	0.0308	0.0000	0.0000
1-Pentene	0.0000	0.0000	0.0000	0.0000	0.0000	0.0093	0.0094	0.0000	0.0000
1-Hexene	0.0000	0.0000	0.0000	0.0000	0.0000	0.0000	0.0000	0.0000	0.0000
1- Decene	0.0000	0.0000	0.0000	0.0000	0.0000	0.0000	0.0000	0.0000	0.0000
Carbon*	0.0000	0.0000	0.0000	0.0000	0.0000	0.0000	0.0000	0.0000	0.0000
Methane	0.0000	0.0000	0.0000	0.0000	0.0000	0.0162	0.0164	0.0000	0.0000
Ethane	0.0000	0.0000	0.0000	0.0000	0.0000	0.0005	0.0005	0.0000	0.0000
Propane	0.0000	0.0000	0.0000	0.0000	0.0000	0.0015	0.0015	0.0000	0.0000
Hydrogen	0.0000	0.0000	0.0000	0.0000	0.0000	0.2454	0.2482	0.0000	1.0000

* Carbon was found to be negative from MATLAB simulations, possibly due to model inaccuracy. As such, carbon composition was removed entirely.

9. References

Argyle, M., & Bartholomew, C. (2015). Heterogeneous Catalyst Deactivation and Regeneration: A Review. *Catalysts,5*(1), 145-269. doi:10.3390/catal5010145

Chan, C., Seville, J, P.K., Baeyens, J. (2010). The Transport Disengagement Height (TDH) in a Bubbling Fluidized Bed (BFB). *Engineering Conferences International*. New York: ECI Digital Archives

Chemical engineering plant cost index (2016). (122)3, pp.84. Access Intelligence, LLC.

Diep, B. T., & Wainwright, M. S. (1987). Thermodynamic equilibrium constants for the methanol-dimethyl ether-water system. *Journal of Chemical & Engineering Data,32*(3), 330-333. doi:10.1021/je00049a015

Element1. (2013). *Methanol Handbook* [Brochure]

Escudero, D., & Heindel, T. J. (2011). Bed height and material density effects on fluidized bed hydrodynamics. *Chemical Engineering Science,66*(16), 3648-3655. doi:10.1016/j.ces.2011.04.036

Forbus, N. P., & Wu, M. M. (1988). *U.S. Patent No. 4777156*. Washington, DC: U.S. Patent and Trademark Office.

Fournol, AB; Bergougnou, M.A. and Baker, C.G.J. (1973) Can. J. Chem. Eng., 51, 401

Geldart, D., & Baeyens, J. (1985). The design of distributors for gas-fluidized beds. *Powder Technology,42*(1), 67-78. doi:10.1016/0032-5910(85)80039-5

H. (2016, December 29). Electricity charges to go up by 5.6% from January to March 2017. Retrieved March 22, 2017, from http://www.straitstimes.com/singapore/electricity-charges-for-first-quarter-to-go-up

Hajimirzaee, S., Ainte, M., Soltani, B., Behbahani, R. M., Leeke, G. A., & Wood, J. (2015). Dehydration of methanol to light olefins upon zeolite/alumina catalysts: Effect of reaction conditions, catalyst support and zeolite modification. *Chemical Engineering Research and Design,93*, 541-553. doi:10.1016/j.cherd.2014.05.011

Edwards, J. (n.d). Keep Cool When Designing Batch Reactors. *Chemical Processing-Jacketed Heating*

Kaarsholm, M., Rafii, B., Joensen, F., Cenni, R., Chaouki, J., & Patience, G. S. (2010). Kinetic Modeling of Methanol-to-Olefin Reaction over ZSM-5 in Fluid Bed. *Industrial & Engineering Chemistry Research,49*(1), 29-38. doi:10.1021/ie900341t

Kaarsholm, M., Joensen, F., Cenni, R., Chaouki, J., & Patience, G. S. (2011). MeOH to DME in bubbling fluidized bed: Experimental and modelling. *The Canadian Journal of Chemical Engineering,89*(2), 274-283. doi:10.1002/cjce.20386

Kunii, D., & Levenspiel, O. (1997). Circulating fluidized-bed reactors. *Chemical Engineering Science,52*(15), 2471-2482. doi:10.1016/s0009-2509(97)00066-3

Kunii, D., & Levenspiel, O. (2012). *Fluidization engineering*. Amsterdam: Elsevier ; Butterworth-Heinemann.

Pierce, M (1998). *Comparing Values of Various Heating Fuels*. Ithaca, New York: Cornell University, Department of Design & Environmental Analysis

Pumpschool (2007). *When to use a Positive Displacement Pump*. Retrieved from: http://www.pumpschool.com/intro/pd%20vs%20centrif.pdf

Seider, W. D., Seader, J. D., Lewin, Daniel R., & Widagdo, S., *Product and Process Design Principles*, John Wiley & Sons, Inc, 2009.

Towler, G., Sinnott, R. K., Sinnott, R. K., & Sinnott, R. K. (2013). *Chemical engineering design: principles, practice, and economics of plant and process design*. Amsterdam: Elsevier.

Turton, R., Bailie, R. C., Whiting, W. B., Shaeiwitz, J. A., & Bhattacharyya, D. (2016). *Analysis, synthesis, and design of chemical processes*. UP, India: Pearson India Education Services.

US Treasury Direct (2017). *Average Interest Rates on U.S Treasury Securities*. Retrieved from: https://www.treasurydirect.gov/govt/rates/pd/avg/avg.htm

Wang, W., Jiang, Y., & Hunger, M. (2006). Mechanistic investigations of the methanol-to-olefin (MTO) process on acidic zeolite catalysts by in situ solid-state NMR spectroscopy. *Catalysis Today,113*(1-2), 102-114. doi:10.1016/j.cattod.2005.11.015

Wen, C. & Yu, Y. (1965). *Mechanics of fluidization*. Chem. Eng. Prog. Symp. Ser.

Werther, J., & Hartge, E. (2004). Modeling of Industrial Fluidized-Bed Reactors. *Industrial & Engineering Chemistry Research,43*(18), 5593-5604. doi:10.1021/ie030760t